buildings

MDPI

Article

Responses of Structural Components of a Full-Scale Nailed Retaining Structure under the Influence of Surcharge Loading and Nail Head Configuration: A Numerical Study

Meen-Wah Gui *,† and Ravendra P. Rajak †

Department of Civil Engineering, National Taipei University of Technology (Taipei Tech), Taipei 106344, Taiwan
* Correspondence: mwgui@ntut.edu.tw
† These authors contributed equally to this work.

Abstract: Soil-nailing is a simple and economical method of stabilizing cut slopes and retaining excavation. Most of the soil-nailing related studies, in particular the experimental work, were conducted in idealized or homogeneous ground, but such a result might not necessarily be representative. Thus, for a more representative study, instead of treating the ground as homogeneous it should be treated as a system of horizontal layers. This study assessed the performance of a full-scale nailed retaining structure for a foundation pit of a 20-storey building through a series of numerical analyses. The influence of full-face facing thickness, nail head geometrical configuration (size and thickness) and surcharge loading on the response of the structural components of the soil-nailing system adopted is the main concern. The results were evaluated in terms of axial force, shear force and bending moment of the structural facing element and the horizontal displacement of the soil retained behind the facing element. In both cases, the distribution of nail axial (tensile) force in each nail reinforcement was also compared and evaluated. It was found that the thickness of full-face facing affected the facing shear force and bending moment, while the surcharge loading influenced the facing axial force and the horizontal displacement of the retained soil and that the magnitude of the axial force registered at the fixed end was governed by the size of the discrete nail head.

Keywords: soil-nailing; nail head; structural facing; excavation; numerical analysis

Citation: Gui, M.-W.; Rajak, R.P. Responses of Structural Components of a Full-Scale Nailed Retaining Structure under the Influence of Surcharge Loading and Nail Head Configuration: A Numerical Study. *Buildings* **2023**, *13*, 561. https://doi.org/10.3390/buildings13020561

Academic Editors: Suraparb Keawsawasvong and Changjie Xu

Received: 11 January 2023
Revised: 9 February 2023
Accepted: 13 February 2023
Published: 18 February 2023

1. Introduction

Soil-nailing became very popular in the last two decades because of its easy installation and economical and speedy construction technique. Using this technique, natural and man-made unstable slopes can be strengthened with the proper installation of steel bars into a slope. Perhaps, the most common method of nail installation is to insert steel bar into a pre-drilled hole and then back-fill the hole with cement-grout under gravitational force or low pressure [1]. Not only temporary or permanent retaining structures can be effectively stabilized using this method, it can also be used in river bank erosion control [2]. In this method, gently inclined boreholes are drilled at required intervals on the slope face and then steel bars are placed and grouted properly with a suitable mix of cement and concrete so that soil nails are covered, and the surrounding soils are well connected to provide sufficient friction in preventing the sliding of the retained soil mass of a slope or excavation.

The soil-nailing method was first carried out in France [3,4] and then slowly spread to various parts of the world because of its performance and easy method of installation. Since then, much field, experimental and analytical work has been carried out to evaluate the performance of soil-nailed structures, e.g., [5–7]. Nails are tensile elements on a slope; the force is transferred to the nails via the friction between the soil and the nails at the time of slope deformation [7–10]. Therefore, the axial tensile force and pullout resistance of a nail play a major role in the performance of a nailed structure [11,12]. As a result, the

study of the mechanical behavior of the nail is important in understanding the stability and strength of a nailed structure of the slope.

Wong et al. [12] studied the field performance of a 9 m deep cut slope and suggested that the soil-nailing technique works effectively for their treated slope. Zhang et al. [13] developed a finite element model that considered soil non-linearity, soil–nail interaction and staged construction for the simulation of the deformation behavior of a nailed cut slope. Smith and Su [5] conducted a series of three-dimensional finite element analysis to study the interaction between soil nails under different service loadings and agreed that soil slope could be well stabilized by the nailing technique. Gui and Ng [9] accomplished a series of 2D and 3D analyses on an instrumented cut slope in Hong Kong using the numerical program FLAC and concluded that the horizontal deflection of their studied slope could be reduced by reducing the horizontal nail spacing, but the grout stiffness did not have any influence on the stability of the study cut slope.

Fan and Luo [14] and Mohamed et al. [15] performed a series of parametric studies to evaluate the effect of nail geometry and orientation on the stability of nail-stabilized slope and confirmed the important roles and contribution of the geometric conditions on the stability of a nailed slope. Using a Plaxis 2D simulation, Ghareh [16] discussed the effect of shear strength and the magnitude of surcharge on the structural behaviour of soil-nailing retaining walls. The variation in the limit equilibrium method (LEM) and the finite element method's (FEM) strength reduction method (SRM) was compared via an analysis of a nailed soil slope by Rawat and Gupta [17], and compared to FEM, it was found that the limit equilibrium method resulted in a higher factor of safety (FOS). However, Wei and Cheng [18] found no major variation in terms of FOS and slip surfaces between the LEM and the SRM; nevertheless, discernible deviation in nail load was found between the SRM and LEM as a result of surcharge variation.

Dai et al. [19], who simulated an earth-retaining structure stabilized by moso bamboo soil nails, concluded that an increase in the soil nails embedment depth rendered an increase in the maximum axial force in the soil nails. Incidentally, Rawat and Gupta [17] also arrived at the same conclusion from their FEM analysis. Experimentally, Mohamed et al. [20] employed a 1:10 pullout model test to study the pull-out force of nail reinforcement and concluded that the nail force decreases as the nail overburden pressure decreases.

Plumelle and Schlosser [3] studied the failure mechanisms of nailed soil walls via three full-scale experiments in France and suggested that slope-facing plays an important role in the face stability of the slopes. There are two types of slope-facing: structural and non-structural facings. The structural facing provides retention action to the ground by its own weight, bending strength or stiffness, while the non-structural facing mainly serves as surface protection from, perhaps, erosion [1]. A centrifuge study of a soil-nailed slope was carried out by Rotte and Viswanadham [21] to study the influence of facing material and nail inclination on the stability of a model nailed slope under seepage conditions. It was found that nail inclination at 10 degrees provides better stability than that of the 25 degrees.

A centrifuge and numerical study were also conducted by Viswanadham and Rotte [22] for a model nailed slope with and without slope facing, and it was found that the slope with rigid facing resulted in a higher value of FOS, while the slope without facing delivered a lower value of FOS. The behavior of nail force distribution with and without the presence of nail head and slope facing has also been studied by [23,24]. For example, Joshi [23] conducted an analytical study on the effect of nail head strength due to the changes in the horizontal S_h and vertical S_v nail spacings and material strength properties and suggested that within the range of $0.8 \leq S_v/S_h \leq 1.0$ the nail head strength increases with the increase of the S_v/S_h ratio.

Based on the results of a series of fieldwork, laboratory work and numerical simulation, Pun and Shiu [25] reported the technological advances of the soil-nailing practice in Hong Kong and outlined the importance of the slope-facing element on the overall stability of the nailed slope where the face and total stability of the nailed slope can be greatly improved by increasing the size of the nail head. Hence, facing elements play an important role in

preventing the stability failure; proper facing elements should be provided to a nailed slope or retaining structure to avoid face failure as well as to increase the overall stability.

Numerical analysis has become much more popular than the traditional method of nail analysis due to the quick analysis process and the increased freedom compared to the trial-and-error approach of analysis. For example, from the FE result of the nature of the shear force and bending moment distribution of nails on a slope, the potential sliding surface of the analyzed slope can be determined [17]. Therefore, FEM is a very useful application to analyze the stability of a nailed wall or any kind of slope stability analysis [26].

The primary goal of this study is to assess the performance of a nailed retaining structure through a series of numerical analyses and to evaluate the influence of facing thickness, nail head geometrical configuration (size and thickness) and surcharge loading on the structural components of the soil-nailing system. The effect of facing thickness and surcharge loading is evaluated in terms of axial force, shear force and bending moment of the structural facing element, while the effect of nail head geometrical configuration is evaluated in terms of horizontal displacement of the retained soil behind the facing. In both cases, the distribution of nail axial (tensile) force in each nail reinforcement is also compared and evaluated. The result of the study allows engineers to sharpen the design method suitable for structural nail head and facing components of a nailed structure.

2. Materials and Methods

The finite element program Plaxis 2D (version 8) was used for the simulation of nail behavior in this study. The simulated problem was indeed a full-scale nailed retaining structure designed for the south wall of a foundation pit of a 20-storey building [27]; the nailed structure was 6.53 m high with a face gradient of 80° from the horizontal. The thickness of the soil layers involved is summarized in Table 1. Because of its long geometry, the problem was simulated by a 22 m by 16 m plane–strain model with mesh boundaries located far enough to minimize the boundary effect on the numerical results [28]. The bottom boundary of the mesh was fixed in both the x- and y-directions, while the left and right vertical boundaries were allowed to move in the vertical direction only. The fine mesh used (Figure 1) was made-up of 15-nodded triangular elements. The soil was assumed to behave as an elastic, perfectly plastic material and characterized by the Mohr–Coulomb failure criterion, while nail, facing and nail head elements were represented by the plate structural elements [29,30] and modeled as elastic materials. The interface between the surrounding soil and the nail was represented via the zero-thickness interface element where its strength parameters are represented via the strength reduction coefficient R_{inter}:

$$R_{\text{inter}} = \frac{c_{\text{inter}}}{c_{\text{soil}}} = \frac{\tan \phi_{\text{inter}}}{\tan \phi_{\text{soil}}} \quad (1)$$

where $(c_{\text{inter}}, \phi_{\text{inter}})$ and $(c_{\text{soil}}, \phi_{\text{soil}})$ are the shear strength parameters of the soil/grout interface and the surrounding soil, respectively. The value of the interface coefficient R_{inter} varies between 0.0 and 1.0, in which $R_{\text{inter}} = 0.0$ is a smooth interface where no shear strength is mobilized, while $R_{\text{inter}} = 1.0$ is a rigid interface where relative displacement between the two materials is disallowed. In practice, the interface coefficient lies between 0.0 and 1.0; the exact value of R_{inter} should be evaluated in the laboratory using a direct shear device. Plaxis [31] recommended that in the absence of detailed information, R_{inter} can be assumed to be of the order of 2/3. As the groundwater table was found well below the sloping face [27] and soil-nailing problems do not normally involve the generation of excess pore-water pressure [14,17,30,32], a drain analysis was conducted.

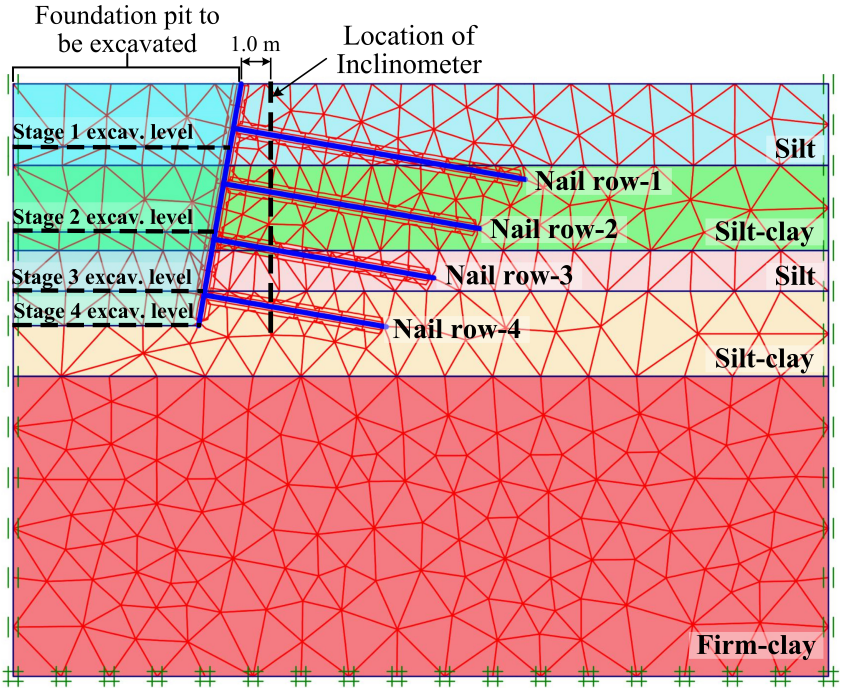

Figure 1. Layout of nail positions, excavation sequences and levels and the finite element mesh adopted in this study.

Table 1. Thickness of soil layers and list of soil parameters used in the numerical simulation.

Soil Layer No.	Soil Types	Thickness (m)	Unit Weight γ (kN/m^3)	Apparent Cohesion c' (kPa)	Internal Friction Angle (°)	Young's Modulus (kPa)
1	Silt	2.2	18.1	14	20	7000
2	Silty clay	2.3	17.9	20	15	12,000
3	Silt	1.1	18.2	15	21	7000
4	Silty clay	2.3	18.2	21	16	14,000
5	Firm clay	8.1	19.0	21	16	26,000

2.1. Method and Materials Properties

Design parameters for nailed structures may be found in FHWA [33,34] and PLAXIS 2D manual guidelines [31]. The thicknesses and properties of the soils of the nailed structure and reinforcement bar used in this study are given in Tables 1 and 2. Soil parameters together with the diameter, yield strength and elastic modulus of reinforcement were extracted from Wang et al. [27], while the elastic modulus of concrete and grout, as listed in Table 2, were essentially the values used by Singh and Babu [30]. A Poisson ratio for soil layers 1–4 was assumed to be 0.3, while that of the fifth layer, which was a firm clay and was included mainly to minimize the bottom boundary effect of the finite element model, was kept at 0.35.

Table 2. List of soil nail and nail head parameters used in the numerical simulation.

Parameter	Value
Yield strength of reinforcement f_y (MPa)	415
Elastic modulus of reinforcement E_n (GPa)	200
Elastic modulus of concrete nail head E (GPa)	34.5
Elastic modulus of grout E_g (GPa)	22
Diameter of reinforcement d (mm)	20
Length of nails (m)	5, 6, 7, 8
Inclination of nail (degree)	10
Horizontal S_h and vertical spacings S_v of nail (m)	1.5
Thickness of facing t (mm)	80, 125, 200, 300
Size of the 100 mm thick nail head (m)	0.2, 0.4 and 0.8
Coefficient of interface R_{inter}	$\frac{2}{3}$

2.2. Axial Stiffness and Flexural Rigidity of Nail and Nail Head

Based on the equivalent-plate-model approach [29,30,35], the axial stiffness $(EA)_n$ and flexural rigidity (bending stiffness) $(EI)_n$ of the nail are given in the following Equation (2):

$$(EA)_n = \frac{E_{eq}}{S_h}\left(\frac{\pi}{4}D_{dh}^2\right) \quad [\text{kN/m}]; \qquad \text{and} \qquad (EI)_n = \frac{D_{dh}^2}{16}\cdot EA \quad [\text{kNm}^2/\text{m}] \tag{2}$$

where S_h is the nails' horizontal spacing, D_{dh} is the diameter of the drilled hole, and E_{eq} is the equivalent elasticity modulus, which accounts for the contribution of elastic stiffness of both the grout cover and the reinforcement bar of the grouted soil nail [30]:

$$E_{eq} = E_n\left(\frac{A_n}{A}\right) + E_g\left(\frac{A_g}{A}\right)$$

where E_n and E_g is the elastic modulus of the nail and the grout, respectively; A is the cross-sectional area of the grouted nail $\left(= 0.25\pi D_{dh}^2\right)$; A_n is the cross-sectional area of the reinforcement bar with diameter d $\left(= 0.25\pi d^2\right)$; and A_g is the cross-sectional area of the grout cover, where $A_g = A - A_n$.

As for the nail head, the axial stiffness rigidity $(EA)_{nh}$ and flexural rigidity $(EI)_{nh}$ may be given by the following Equation (3) [24]:

$$(EA)_{nh} = \frac{E}{S_h}\cdot t_{nh}\cdot n_{nh} \qquad \text{and} \qquad (EI)_{nh} = \frac{n_{nh}^2}{12}\cdot EA \tag{3}$$

where t_{nh} is the thickness of the nail head, n_{nh} is the size of the square nail head, and E is the elastic modulus of the facing and nail head material. The axial stiffness $(EA)_{face}$ and flexural $(EI)_{face}$ rigidity of the facing element were given by Garzón-Roca et al. [32] in Equation (4):

$$(EA)_{face} = Et_{face} \qquad \text{and} \qquad (EI)_{face} = \frac{Et_{face}^3}{12} \tag{4}$$

In the simulation, after generating the 2D FE mesh, the initial stresses of the model are computed using the k_0 procedure based upon Jaky's [36] relation ($k_0 = 1 - \sin\phi$). The excavation was then conducted in four stages to reach the bottom of the foundation pit, which is at the depth of 6.53 m. Excavation was simulated by deactivating the soil element, while installation was simulated by activating the relevant structural elements. The global FOS was determined by using the $\phi - c$ strength reduction technique available in the program where the shear strength parameters of the soil are gradually reduced until the slope collapses. The four stages of construction sequences are shown in Figure 1 and briefly described here:

1. Stage 1: Excavate to EL −1.70 m, and install the first-level nailing (Nail row–1) at EL −1.20 m and nail head NH01/facing.
2. Stage 2: Excavate to EL −3.20 m, and install the second-level nailing (Nail row–2) at EL −2.70 m and nail head NH02/facing.
3. Stage 3: Excavate to EL −4.70 m, and install the third-level nailing (Nail row–3) at EL −4.20 m and nail head NH03/facing.
4. Stage 4: Excavate to EL −6.53 m, and install the fourth-level nailing (Nail row–4) at EL−5.7 m and nail head NH04/facing.

3. Results and Discussion

3.1. Analysis of Unsupported Excavation Face

Initially, a numerical analysis was performed by assuming the foundation pit was excavated without any soil-nailing support. The FOS obtained was 1.02, which was very close to the critical value of 1, and thus the excavated face could be deemed as unsafe. Figure 2a shows the result of the distribution of total displacements of the retained soil at the end of foundation pit excavation; it also provides an indication of the possible location of the critical slip surface in the event of a sliding failure.

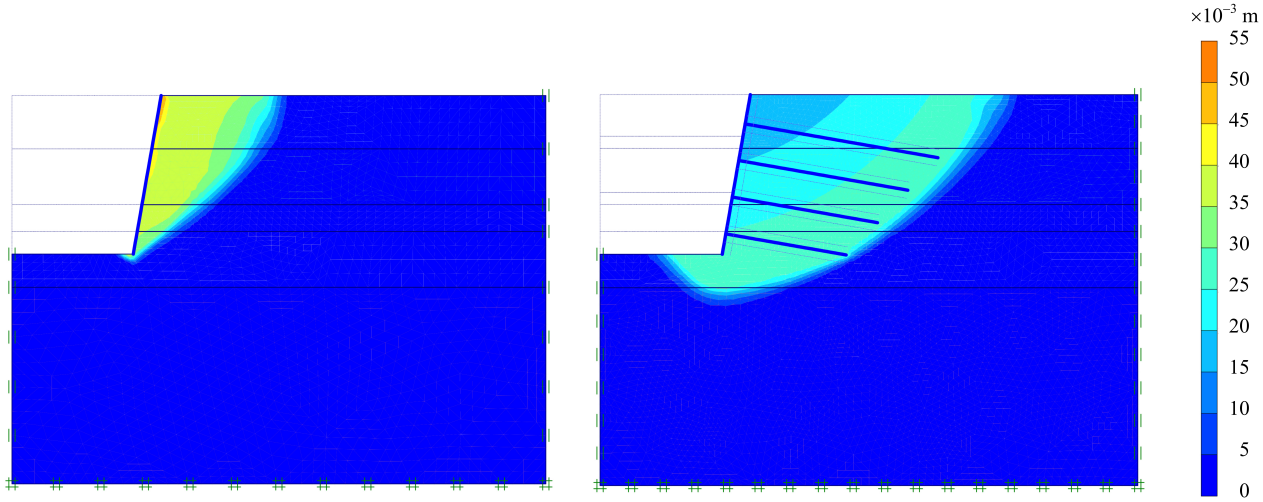

Figure 2. Distribution of total displacements for the case of: (**a**) excavation without soil-nailing support; (**b**) excavation with soil-nailing support, and their corresponding critical sliding surface.

In the following analyses, four rows of soil-nailing, as shown in Figure 1, have been provided. The lengths of the nails have been arranged in such a way that they all pass through the possible sliding surface shown in Figure 2a, which was 8 m, 7 m, 6 m and 5 m, respectively, from top (Nail row–1) to bottom (Nail row–4). With this sort of arrangement, the total required length was 26 m, which is less than the 34 m used in [27]. Even though the consumption of the reinforcement bar was 23.5% less than that used by [27]; the FOS obtained (FOS = 1.53) was still 50% higher than that in the case of excavation without soil-nailing. Figure 2b shows the result of the distribution of total displacements of the retained soil at the end of pit excavation for the case of excavation with soil-nailing support. The critical slip surface in this case is seen located beyond the lengths of the soil nails; in general, as the sliding mass enlarges, its FOS increases, and its stability also improves.

During the analysis, the effect of facing thickness, surcharge, nail head size and thickness were considered and analyzed. The results were presented in terms of facing axial force, shear force, and bending moment. In addition, the retained soil displacement profile recorded by the inclinometer installed 1 m behind the wall (Figure 1) was also presented.

3.2. Effect of Facing Thickness

To study the effect of facing thickness on the behavior of the nailed structure, various thicknesses of facing were considered here, i.e., 80, 125, 200 and 300 mm; no surcharge loading was applied in this case. The results for the effect of facing thickness on facing axial force, shear force, bending moment and retained soil displacement with depth are presented in Figure 3. Figure 3a shows the profile of the facing axial force with depth; in general, the axial force remains reasonably unaffected by the facing thickness except in the silty-clay layer between the depths of −2.70 m and −5.20 m, which revealed that the axial force increased slightly with the increase of facing thickness. The axial force was zero at the top of the facing, while the maximum axial force was observed at the bottom of the facing. The increase of axial force with depth was most likely due to the transfer of the normal stress of the nail to the structural facing element [16].

Figure 3b,c, respectively, present the distribution of shear force and bending moment along the height of the facing. The values of maximum shear force and maximum bending moment are the two values required for the safe design of concrete facing. It is observed that as the facing thickness increase, the shear force and bending moment also increase. The maximum values of shear force and bending moment occurred in the case of 300 mm thick facing. The contribution of soil-nailing is seen, whereby it prevented the shear force and the bending moment of the facing from increasing continuously at the elevation of the nails.

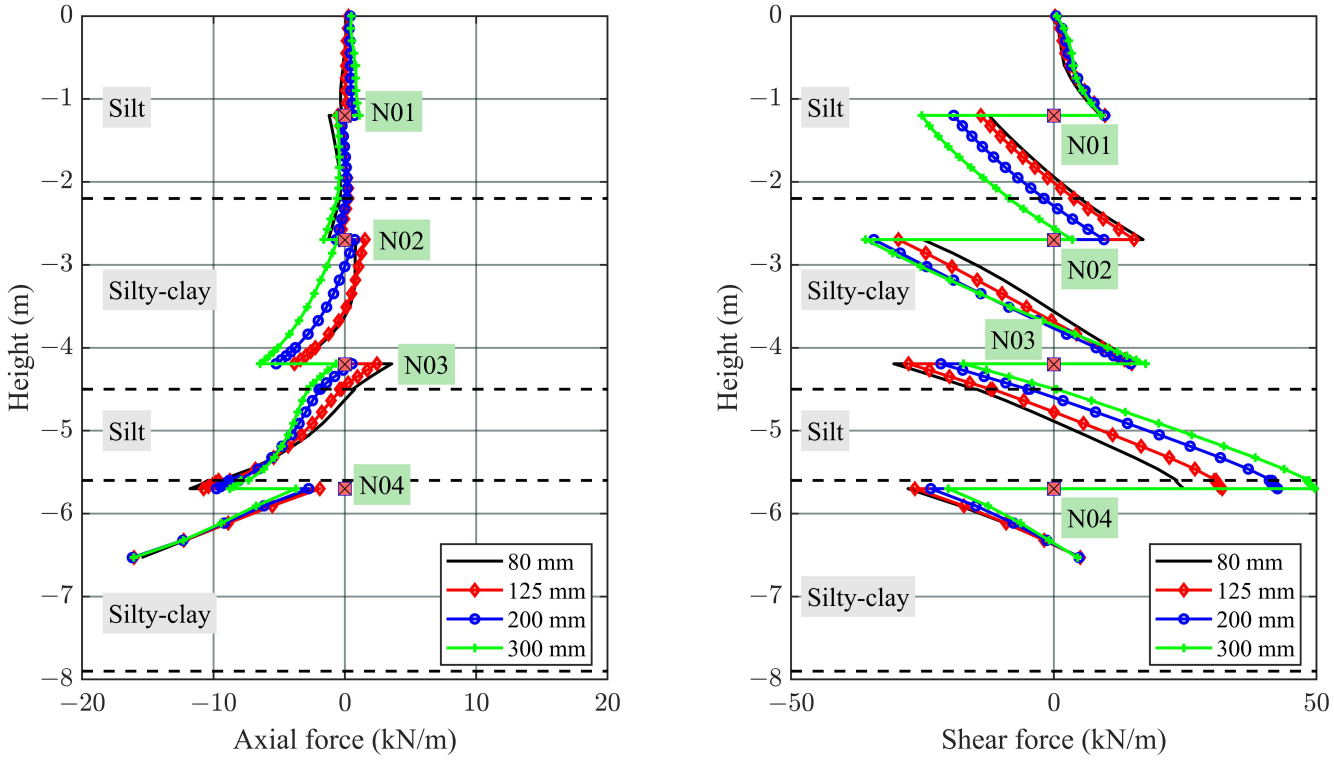

(**a**) (**b**)

Figure 3. *Cont.*

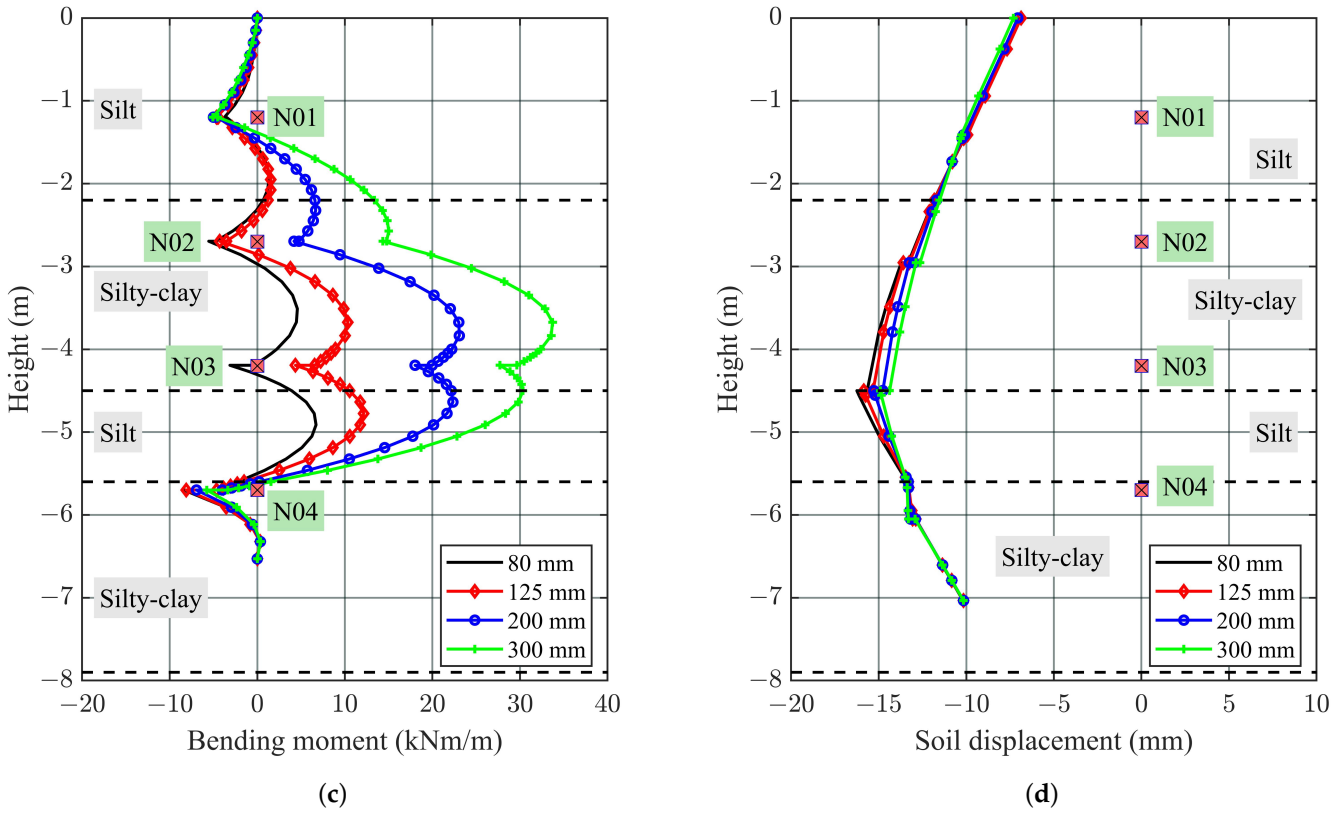

Figure 3. Facing thicknesses and responses of facing in terms of: (**a**) axial force; (**b**) shear force; (**c**) bending moment; (**d**) retained soil displacement.

Figure 3d shows the horizontal displacement of the soil behind the nailed structure. The retained soil displacement was recorded one meter behind the facing as shown in Figure 1; the displacement increased to a maximum value at a depth of about 70% of the excavation depth, which is just below nail row No. 3 (N03). Thereafter, the displacement decreased until the level of the excavation. It was found that the facing thickness has an insignificant effect on the horizontal displacement of the soil. Rowe and Ho [37] and Vieira et al. [38] who studied the influence of facing rigidity on a reinforced soil retaining wall also concluded that the maximum horizontal displacement reduces slightly with the increase in value of rigidity (thickness). It was also observed that the sliding surface moved away from the excavated face when the facing thickness was increased.

The distribution of nail axial (tensile) forces was also recorded during the numerical analysis. A typical distribution of nail axial force without any surcharge loading acting on the ground surface is presented in Figure 4. In general, the value of the axial force increased with the increase in facing thickness except for nail row three (N03). This could be due to the variation of axial forces generated in the facings, as shown in Figure 3a, in which the facing axial force is higher in the case of 80 mm thick facing than that of the 300 mm thick facing as a result of the "pull-back" effect by nail N03. It was also observed that for a particular thickness, the value of the tensile force in the nail installed in the top row (Nail row–1) was smaller than that in the nail installed in the lowest row (Nail row–4). Viswanadham and Rotte [22], who performed centrifuge simulation, also found that in the case of stiff facing, the nail tensile force increased from the upper row to the lower row nails. The observation is in agreement with the finding of Dai et al. [19] in which they claimed that an increase in the nail embedment depth rendered an increase in the maximum axial force in the nail; thus, the lowest row of nails has the maximum tensile axial force.

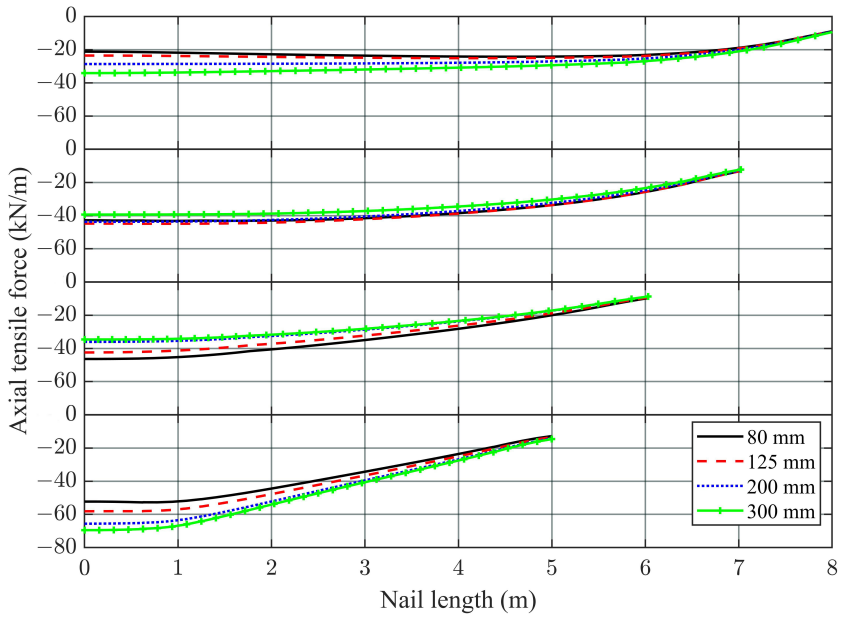

Figure 4. Distribution of nail axial force with various facing thicknesses.

Figure 5 shows the total nail tensile force recorded at the joint between the facing and the nails for all thicknesses of facing. The result from this study showed that the total nail tensile force on the facing increased slightly with the increase of facing thickness. As the facing thickness increased from 80 mm to 300 mm, the total nail force only increased by about 15 kN.

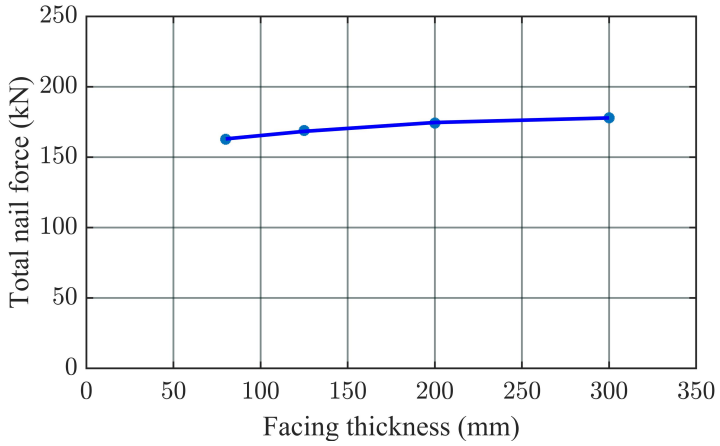

Figure 5. Total nail force recorded on the facing for each facing thickness.

3.3. Effect of Surcharge Loading

Three uniformly distributed surcharge loadings: 10, 20 and 30 kPa were applied full width to the ground surface of the nailed structure, and its effect on the responses of the structural facing was examined (Figure 6). For this study, the facing thickness was kept constant at 80 mm. Figure 6a shows the distribution of the facing axial force with depth and under the surcharge loadings of 0, 10, 20 and 30 kPa; the results obviously indicate that the facing axial force increased with the increase of the surcharge loading. As the surcharge increased, the lateral earth pressure also increased, and the pressure eventually transferred to the facing element. There is a jump, i.e., decrease of axial force, at the elevation of the nail heads. This indicates that the nails played a role in restraining the development of facing axial force. The facing and the nails were rigidly connected so that during loading

the force from the nails can be transferred to the facing. In addition, it was observed that the facing axial force increased with the facing depth.

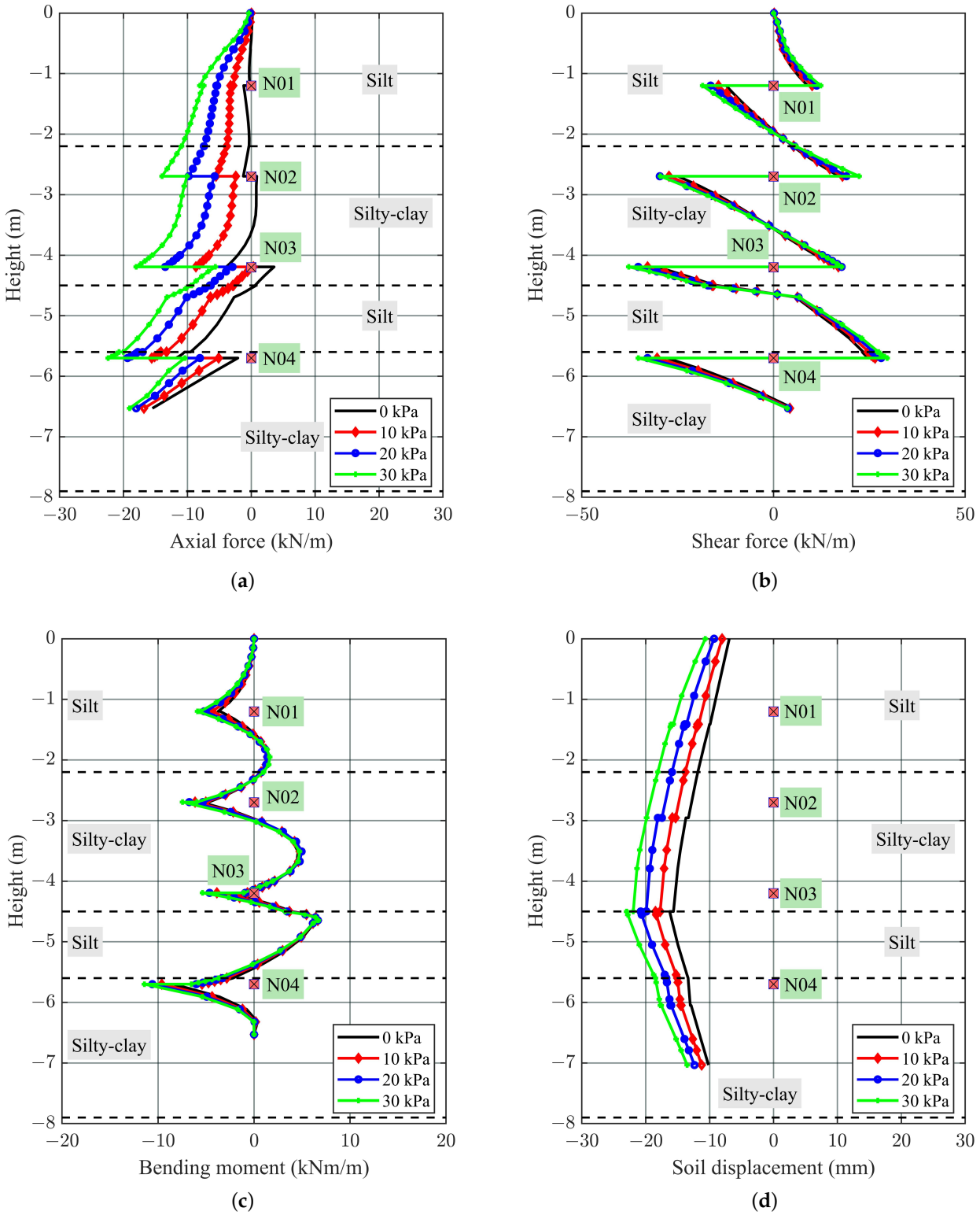

Figure 6. Surcharge loadings and responses of facing in terms of: (**a**) axial force; (**b**) shear force; (**c**) bending moment; (**d**) retained soil displacement.

Figure 6b,c show the distribution of shear force and bending moment, respectively, of the facing with depth under the considered surcharge loadings. In this case, the shear force

and bending moment of the facing remained reasonably unchanged or increased minutely with the increase of surcharge loading when it was subjected to a surcharge loading of between 0 and 30 kPa. Nevertheless, the results show that the maximum shear force and bending moment occurred at the elevation of the nail in the lowest row (Nail row–4). As such, the joint between the nail and the facing should be designed carefully to avoid facing connection failure. The soil horizontal displacement profile, which was recorded one meter behind the facing, is plotted in Figure 6d. The result shows that with the higher value of surcharge load, the retained soil displacement also increases. The maximum displacement was observed at the interface between the second layer silty clay and the third layer silt at EL −4.5 m, about 70% of excavated depth, when a 30 kPa surcharge load was acting full width on the ground surface. The results in this study were found to be similar to the work conducted by Ghareh [16].

The distribution of axial forces along the nails was also observed and shown in Figure 7. The results show that the nail axial force increased with the increase of surcharge loading. Again, the maximum nail tensile force was found to be in the most bottom nail for the surcharge of 30 kPa, and the minimum value of nail axial force was found in the nail in the top row when there was no surcharge loading acting on the ground surface.

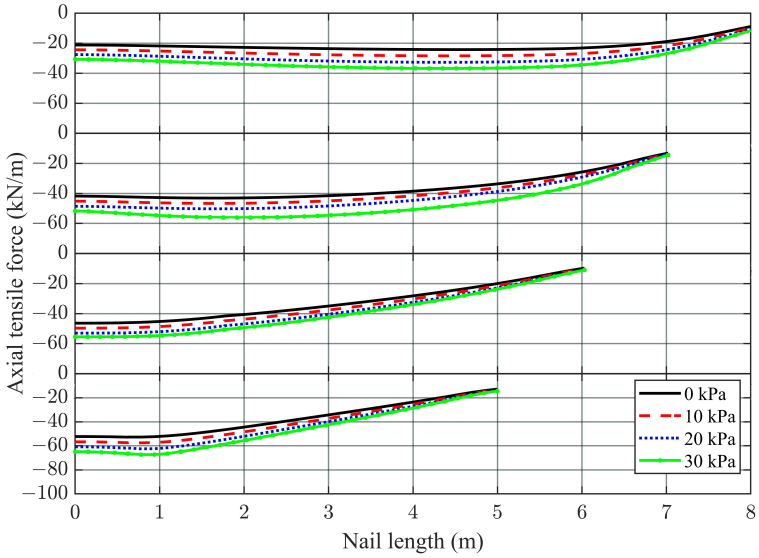

Figure 7. Distribution of nail axial force under various surcharge loadings.

3.4. Effect of Soil Nail Head Size

To enhance the mobilization of tensile resistance of soil nails, nails are commonly fixed to soil nail heads on the surface of the slope or excavated face. They are important elements in the soil-nailing system as they prevent face failure, limit soil erosion and contribute to the overall strength and stability of the slope and nailed structure. Soil nail heads can be isolated concrete pads or integrated into grillage beams or even a shotcrete facing, and its strength depends on various factors, such as nail spacing, nail length, nail angle, slope angle and shear strength of the soil concerned [23]. In this study, isolated concrete pads for soil nails were examined; three different sizes of the nail head, i.e., 200 mm, 400 mm and 800 mm as per the FHWA [34] nailing manual, together with the cases of with and without facing were analyzed. The facing element covers the full-face of the excavated face. For a meaningful comparison of results, the thickness of these nail heads was kept at 100 mm.

The distribution of nail axial force for nail heads of various sizes and facing element is shown in Figure 8; the figure shows that as the size of the constant thickness nail head increases, the nails tensile force, in particular within the first 2 m of the nail length from the nail head, also increase for all the nails. The nature of the distribution of the nails axial force in the case of facing is different from that using nail heads, Figure 9; the end force in

the case of nails rigidly connected to the facing is larger (Figure 9a) than that connected to a smaller size nail head (Figure 9b). It can be seen from Figure 8 that if there was no facing element or nail head used, the end force of the nail was zero on the excavated face for nails in all the rows, which was plausible as no reaction force (Newton's Third Law) could be generated at this end to counter the nail force. With the use of nail heads, the value of the nails axial force on the excavated face increased with the increase of the size of the nail head. Thus, in the case of facing element or nail heads, the nails would somehow be fixed to the excavated face and in turns be able to provide the reaction required to sustain the nail tensile force. The use of larger nail heads would sustain more nail force; thus, higher nail tensile force could be seen mobilized on the excavated face. Figure 8 also revealed that as the depth of each row of nails increased, the position of the maximum axial force moved towards the excavated face.

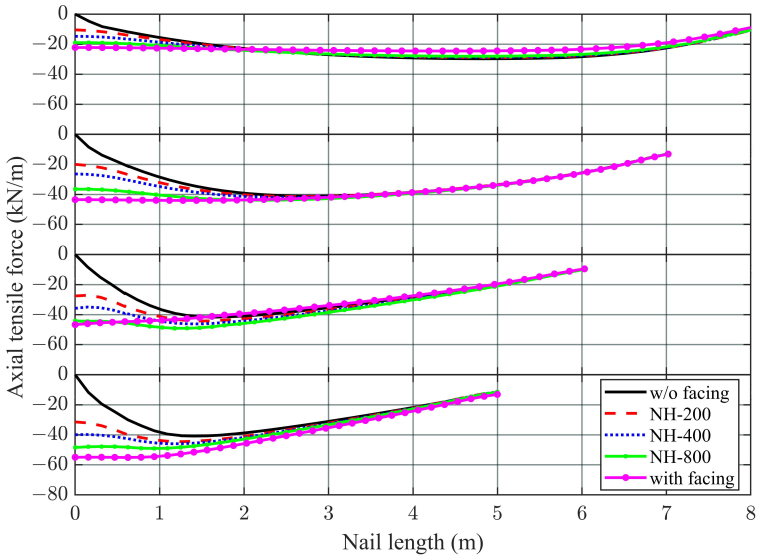

Figure 8. Distribution of nail axial force for nail heads of various sizes and facing element.

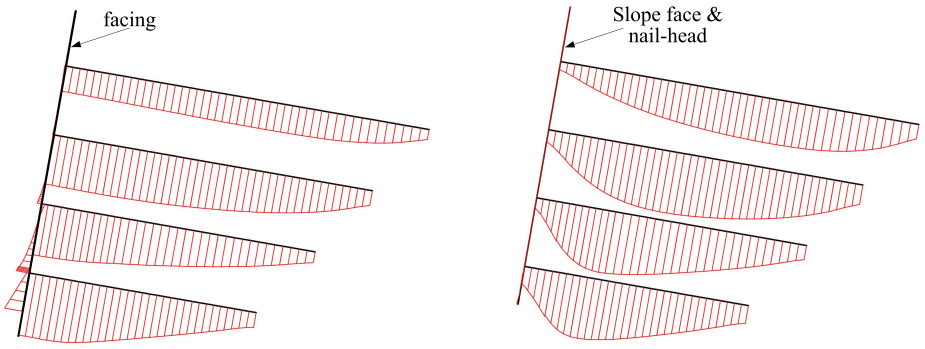

Figure 9. Distribution of nails axial force with excavated face covers by: (**a**) full-face facing; (**b**) nail head.

Figure 10 presents the soil horizontal displacement profiles generated under nail heads of various sizes and with and without the use of a facing element. In general the magnitude of the displacement reduces as the nail head size increases; the minimum displacement profile was obtained when the excavated face was protected by a full-face facing element. Therefore, full-face facing element provided better stability to the excavated face and nailed structure than that provided by the discrete nail heads.

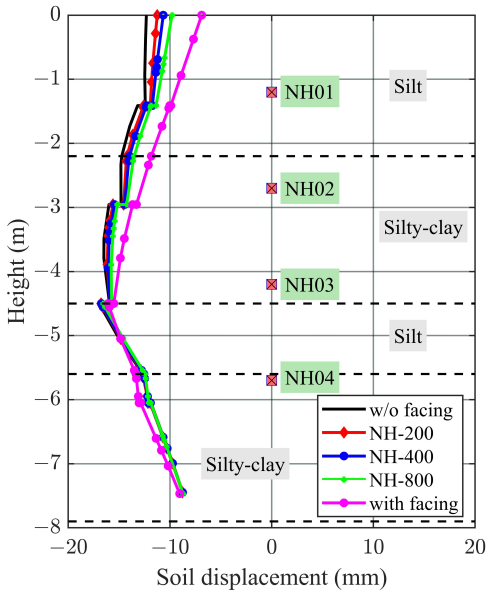

Figure 10. Retained soil displacement profiles generated under nail heads of various sizes and with and without the use of a facing element.

3.5. Effect of Nail Head Thickness

The current finite element study was also conducted to examine the effect of nail head thicknesses on the response of the structural nail head element. In this analysis, the size of the nail head was kept constant at 800 mm, while three different thicknesses were considered: 100 mm, 200 mm and 500 mm. Figure 11 shows the distribution of nail axial force obtained using nail heads with three difference thicknesses. The figure shows that there is no variation at all in the nails axial force for the three different thicknesses of nail head. Figure 12 presents the horizontal displacement profile with the depth of the retained soil; as in the case of nail axial force, there is no significant difference found in these profiles, nor for the three different nail head thicknesses. According to the reference manual of FHWA [33] and Shiu and Chang [39], a nail head attracts force from the respective nail and the face soil that made contact with the nail head. By increasing the thickness of the nail head, the contact area between the nail head and the soil remained the same since their size is essentially the same. As long as the thickness of the nail head is sufficiently provided to resist shear force, it is unnecessary to adopt a thicker nail head. Thus, the nail head thickness and the stability of the nailed structure have no direct connection.

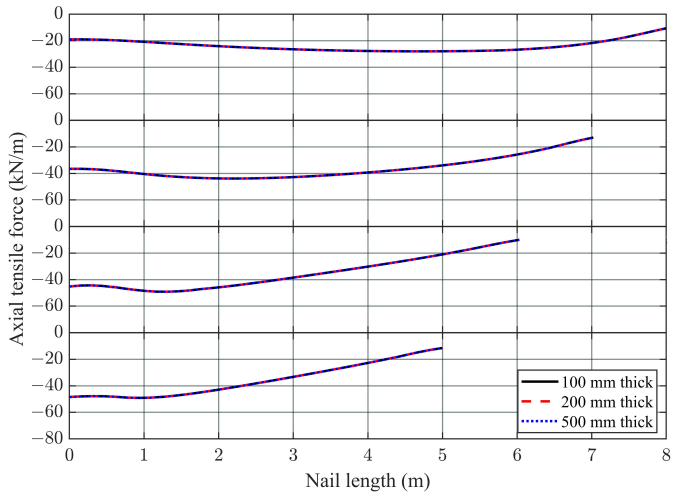

Figure 11. Distribution of nail axial force under nail heads of various thicknesses.

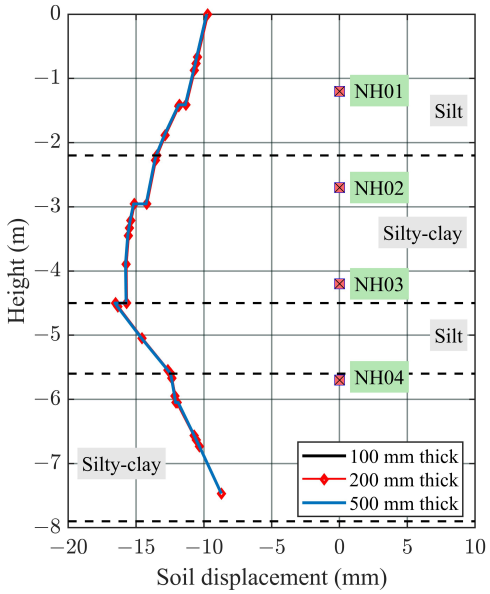

Figure 12. Retained soil displacement profiles under nail heads with various thicknesses.

3.6. Surcharge, Maximum Nail Force and Vertical Settlement of Ground Surface

It is necessary to know the surcharge–vertical settlement response of the nailed structure, in particular for monitoring its long-term performance. However, only a few experimental and numerical studies have been conducted in the past [15,40]. To understand the load–settlement behavior better, a series of surcharge loading, such as 5, 10, 15, 20, 25 and 35 kPa were applied full width on top of the ground surface. For every surcharge loading, vertical settlement on the ground surface of the retained structure was recorded 1 m behind the excavated face. The surcharge load–settlement result is plotted and presented in Figure 13a. From the load–settlement response, it can be observed that as the surcharge loading increased, the ground vertical settlement increased; a maximum settlement of 21 mm was recorded for the surcharge loading of 35 kPa.

The response of maximum nail force on the vertical settlement of the ground surface of the nailed structure is important in understanding the mechanical behavior of soil nails of a nailed structure. A series of surcharge loadings, from 5 kPa to 35 kPa, was applied to the ground surface of the nailed structure. The excavated face was covered by a 80 mm thick full-face facing.The corresponding vertical settlement of the under-loading ground surface is plotted in Figure 13a. It is obvious that the vertical settlement increased with the

increase of surcharge loading. The maximum axial force of each nail from rows–1 to 4 was recorded, together with the corresponding vertical settlement of the ground surface were plotted in Figure 13b. It is observed that the ground surface vertical settlement increased linearly with the maximum nail axial force of the nailed structure and that the maximum nail force of 70 kN/m was seen in the nail located in the most bottom row–4 and with a corresponding vertical settlement of about 21 mm. The variation of the maximum axial force in the nails of row–2 and 3 was found to be smaller than that between the nails in rows–1 and 2, the reason is not quite obvious, but incidentally both the nails of row–2 and 3 were located in the same soil layer. Hence, the result revealed that the vertical settlement of the ground surface where the surcharge loading was acting is linearly related to the maximum nail axial force but non-linearly related to the embedment depth of the nails.

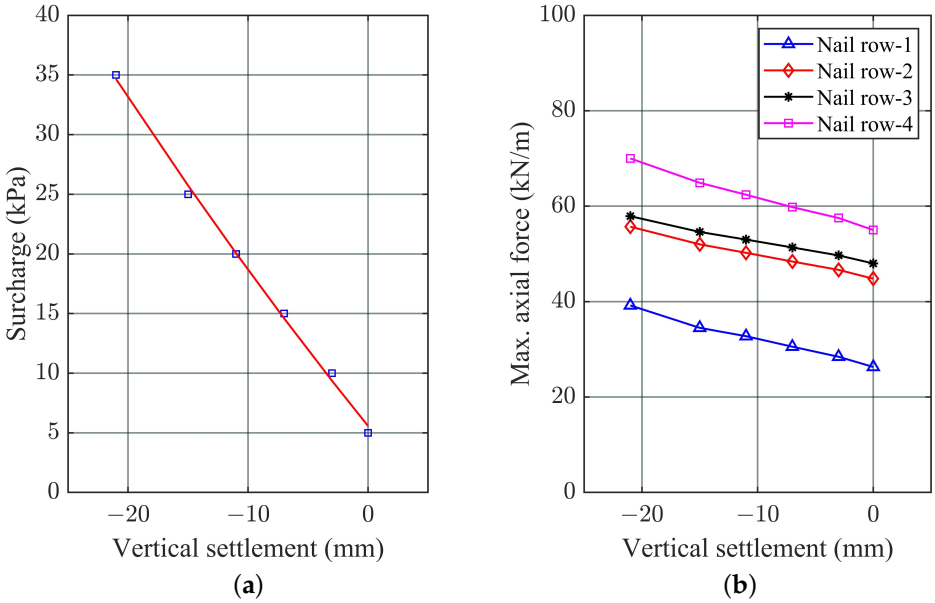

Figure 13. Relation between: (**a**) surcharge; (**b**) maximum nail tensile force, with ground surface vertical settlement.

4. Conclusions

In this study, the performance of a nailed structure for an excavated foundation pit was studied. The excavation face was supported by four rows of soil nails. The influence of different facing thicknesses, surcharge loadings and nail head geometrical configurations on the nailed structural components were examined. The facing thicknesses considered were 80, 125, 200 and 300 mm; the nail head sizes were 200, 400 and 800 mm; the surcharge loadings were 10, 20 and 30 kPa. The analyses were performed by considering the joint of the studied nails was rigidly connected to (i) full-face facing, (ii) nail head of various sizes and thicknesses, and (iii) freely exposed, i.e., without facing and nail head. The responses of the structural facing element were evaluated in terms of axial force, shear force and bending moment, while the response of the excavated face was evaluated based upon the horizontal displacement of the retained soil. Based on the results from this parametric study, the following conclusions were made:

1. Increasing facing thickness has obvious influence on the facing shear force and bending moment, but it only has a slight or perhaps negligible influence on the facing axial force and soil horizontal displacement.
2. Surcharge loading did not seem to have any influence on the facing shear force and bending moment, but as surcharge loading increases, both the facing axial force and soil horizontal displacement increase. The maximum horizontal displacement was found to be mobilized at about 70% of excavated depth. It was observed that the

maximum nail axial force increases with the increase of nail embedment depth from top to bottom. The sum of all four nail axial forces acting on the facing also increased with the increase of surcharge loading.

3. Nail axial force at the fixed end on the excavated face was found to increase with the increase of nail head size, with the maximum value being observed in the case of full-face facing. Conversely, the horizontal displacement of the retained soil reduces as the nail head size increases with the minimum displacement profile being obtained when the excavated face was protected by a full-face facing. In other words, as the nail head size increases, the overall stability of the retained soil also increases. Although full-face facing provided the highest overall stability, particular attention must be paid to the design of the nail reinforcement such that the mobilized axial force is still within the reinforcement's tensile capacity.
4. Changing nail head thickness has no effect on the nail axial force and the horizontal displacement of the retained soil.
5. Vertical settlement of the ground surface, on which the surcharge loading was acting, was found to be linearly related to the maximum nail axial (tensile) force but not the nail embedment depth.

More work on mechanical properties of nailed structures, combined with the effect of reinforcement bar and soil properties would be necessary before the soil-nailing advantage could be realized in practice.

Author Contributions: Conceptualization, R.P.R. and M.-W.G.; numerical analysis, R.P.R.; numerical data curation, R.P.R.; writing—original draft preparation, R.P.R.; writing—review and editing, M.-W.G.; supervision, M.-W.G. All authors have read and agreed to the published version of the manuscript.

Funding: This research received no external funding.

Institutional Review Board Statement: Not applicable.

Informed Consent Statement: Not applicable.

Data Availability Statement: Not applicable.

Acknowledgments: We would like to thank the three anonymous Reviewers for taking the time and effort necessary to review the manuscript and sincerely appreciate all insightful comments and suggestions, which helped us to improve the quality of the manuscript.

Conflicts of Interest: The authors declare no conflict of interest.

Abbreviations

The following abbreviations are used in this manuscript:

FEM	Finite element method
FHWA	Federal Highway Administration
FOS	Factor of safety
LEM	Limit equilibrium method
NH	Nail head
SRM	Strength reduction method

References

1. GEO. *Guide to Soil Nail Design and Construction: Geoguide 7*; Geotechnical Engineering Office, The Government of the Hong Kong, Special Administrative Region: Hong Kong, 2008; 100p.
2. Mittal, S., Biswas, A.K. River bank erosion control by soil nailing. *Geotech. Geol. Eng.* **2006**, *24*, 1821–1833. https://doi.org/10.1007/s10706-006-7127-6.
3. Plumelle, C.; Schlosser, F. A French National Research Project on Soil Nailing: CLOUTERRE. *Perform. Reinf. Soil Struct.: Proc. of Int. Reinforced Soil Conf.* **1990**, British Geotechnical Society, Glassgow, 219–223.
4. Schlosser, F.; Plumelle, C.; Unterreiner, P.; Benoît, J. Failure of a full scale experimental soil-nailed wall by reducing the nails lengths (French Research Project CLOUTERRE). *Proc. of Int. Conf. Earth Reinf. Pract., IS Kyushi'92*, **1992**, *1*, 531–535.

5. Smith, I.M.; Su, N. Three-dimensional FE analysis of a nailed soil wall curved in plan. *Int. J. Numer. Anal. Methods Geomech.* **1997**, *21*, 583–597. https://doi.org/10.1002/(SICI)1096-9853(199709)21:9<583::AID-NAG831>3.0.CO;2-K.
6. Turner, J.P.; Jensen, W.G. Landslide stabilization using soil nail and mechanically stabilized earth walls: Case study. *J. Geotech. Geoenvironmental Eng.* **2005**, *131*, 141–150. https://doi.org/10.1061/(ASCE)1090-0241(2005)131:2(141).
7. Li, J.; Tham, L.G.; Junaideen, S.M; Yue, Z.Q.; Lee, C.F. Loose fill slope stabilization with soil nails: Full-scale test. *J. Geotech. Geoenvironmental Eng.* **2008**, *134*, 277–288.
8. Duncan, J.M. State of the art: Limit equilibrium and finite element analysis of slopes. *J. Geotech. Eng.* **1996**, *122*, 577–596.
9. Gui, M.W.; Ng, C.W.W. Numerical study of nailed slope excavation. *Geotechnical Engineering*. *J. Seags Agssea* **2006**, *37*, 1–12. Available online: http://seags.ait.asia/e-journal/1970-2012/GEJ_2006_v37n1_April.pdf (accessed on 22 February 2022).
10. Rawat, S.; Gupta, A.K.; Kumar, A. Pullout of soil nail with circular discs: A three-dimensional finite element analysis. *J. Rock Mech. Geotech. Eng.* **2017**, *9*, 967–980. https://doi.org/10.1016/j.jrmge.2017.05.003.
11. Zhou, W.H.; Yuen, K.V.; Tan, F. Estimation of maximum pullout shear stress of grouted soil nails using Bayesian probabilistic approach. *Int. J. Geomech.* **2013**, *13*, 659–664. https://doi.org/10.1061/(ASCE)GM.1943-5622.0000259.
12. Wong, I.H.; Low, B.K.; Pang, P.Y.; Raju, G.V.R. Field performance of nailed soil wall in residual soil. *J. Perform. Constr. Facil.* **1997**, *11*, 105–112. https://doi.org/10.1061/(ASCE)0887-3828(1997)11:3(105).
13. Zhang, M.J.; Song, E.X.; Chen, Z.Y. Ground movement analysis of soil nailing construction by three-dimensional (3-D) finite element modeling (FEM). *Comput. Geotech.* **1999**, *25*, 191–204. https://doi.org/10.1061/(ASCE)1090-0241(2008)134:3(277).
14. Fan, C.C.; Luo, J.H. Numerical study on the optimum layout of soil–nailed slopes. *Comput. Geotech.* **2008**, *35*, 585–599. https://doi.org/10.1016/j.compgeo.2007.09.002.
15. Mohamed, M.H.; Ahmed, M.; Mallick, J.; Hoa, P.V. An experimental study of a nailed soil slope: Effects of surcharge loading and nails characteristics. *Appl. Sci.* **2021**, *11*, 4842. https://doi.org/10.3390/app11114842.
16. Ghareh, S. Parametric assessment of soil-nailing retaining structures in cohesive and cohesionless soils. *Measurement* **2015**, *73*, 341–351. https://doi.org/10.1016/j.measurement.2015.05.043.
17. Rawat, S.; Gupta, A.K. Analysis of a nailed soil slope using limit equilibrium and finite element methods. *Int. J. Geosynth. Ground Eng.* **2016**, *2*, 1–23. https://doi.org/10.1007/s40891-016-0076-0.
18. Wei, W.B.; Cheng, Y.M. Soil nailed slope by strength reduction and limit equilibrium methods. *Comput. Geotech.* **2010**, *37*, 602–618. https://doi.org/10.1016/j.compgeo.2010.03.008.
19. Dai, Z.H.; Gup, W.D.; Zheng, G.X.; Ou, Y.; Chen, Y.J. Moso bamboo soil-nailed wall and its 3D nonlinear numerical analysis. *Int. J. Geomech.* **2016**, *16*, 04016012. https://doi.org/10.1061/(ASCE)GM.1943-5622.0000634.
20. Mohamed, M.H.; Ahmed, M.; Mallick, J. Pullout behavior of nail reinforcement in nailed soil. *Appl. Sci.*, **2021**, *11*, 6419. https://doi.org/10.3390/app11146419.
21. Rotte, V.M.; Viswanadham, B.V.S. Influence of nail inclination and facing material type on soil-nailed slopes. *Proc. Inst. Civ.-Eng.-Ground Improv.* **2013**, *166*, 86–107. https://doi.org/10.1680/grim.11.00026.
22. Viswanadham, B.V.S.; Rotte, V.M. Effect of facing type on the behaviour of soil-nailed slopes: Centrifuge and numerical study. *Discovery*, **2015**, *46(215)*, 214–223. http://www.discoveryjournals.org/discovery/current_issue/v41-46/n186-215/A201.pdf?.
23. Joshi, B. Behavior of calculated nail head strength in soil-nailed structures. *J. of Geotechnical and Geoenvironmental Engineering*, **2003**, *129*, 819–828. https://doi.org/10.1061/(ASCE)1090-0241(2003)129:9(819).
24. Kaothon, P.; Chhun, K.T.; Yune, C.Y. Numerical evaluation on steep soil-nailed slope using finite element method. *Int. J. of Geo-Eng.*, **2021**, *12*, 299–309. https://doi.org/10.1186/s40703-021-00159-y.
25. Pun, W.K.; Shiu, Y.K. Design practice and technical developments of soil nailing in Hong Kong. In *Geotechnical Advancements in Hong Kong Since 1970s: Proceedings of the HKIE Geotechnical Division 27th Annual Seminar*; Hong Kong Institution of Engineers, Geotechnical Division: Hong Kong, 2007; Volume 197, p. 212. Available online: https://hkss.cedd.gov.hk/hkss/filemanager/common/publications-resources/list-of-technical-papers/220_Pun%20&%20Shiu%20(2007)_Design%20practice%20and%20technical%20developments%20of%20soil%20nailing%20in%20Hong%20Kong.pdf (accessed on 22 February 2022).
26. Johari, A.; Hajivand, A.K.; Binesh, S.M. System reliability analysis of soil nail wall using random finite element method. *Bull. Eng. Geol. Environ.* **2020**, *79*, 2777–2798. https://doi.org/10.1007/s10064-020-01740-y.
27. Wang, H.; Cheng, J.; Li, H.; Dun, Z.; Cheng, B. Full-scale field test on construction mechanical behaviors of retaining structure enhanced with soil nails and prestressed anchors. *Appl. Sci.*, **2021**, *11*, 7928. https://doi.org/10.3390/app11177928.
28. Briaud, J.L.; Lim, Y.J. Soil-nailed wall under piled bridge abutment: Simulation and guidelines. *J. Geotech. Geoenvironmental Eng.* **1997**, *123*, 1043–1050. https://doi.org/10.1061/(ASCE)1090-0241(1997)123:11(1043).
29. Sivakumar Babu, G.L.; Singh, V.P. Simulation of soil nail structures using PLAXIS 2D. *Plaxis Bull.* , **2009**, *25*, 16–21. Available online: https://communities.bentley.com/cfs-file/__key/communityserver-wikis-components-files/00-00-00-01-05/Iss25_5F00_Art3_5F002D005F00_Simulation_5F00_of_5F00_Nail_5F00_Structures.pdf (accessed on 22 February 2022).
30. Singh, V.P.; Sivakumar Babu, G.L. 2D numerical simulations of soil nail walls. *Geotech. Geol. Eng.*, **2010**, *28*, 299–309. https://doi.org/10.1007/s10706-009-9292-x.
31. *Plaxis 2D—Version 8: Reference Manual*; Delft University of Technology: Delft, The Netherlands, 2002.

32. Garzón-Roca, J.; Capa, V.; Torrijo, F.J.; Company, J. Designing soil-nailed walls using the Amherst wall considering problematic issues during execution and service life. *Int. J. Geomech.*, **2019**, *19*, 05019006. https://doi.org/10.1061/(ASCE)GM.1943-5622.0001453.
33. Lazarte, C.A.; Robinson, H.; Gomez, J.E.; Baxter, A.; Cadden, A.; Berg, R. Geotechnical Enginering Circular No 7: Soil Nail Walls, Reference Manual. Publication No. FHWA-NHI-14-007. U.S. Department of Transportation Federal Highway Administration , 2015. Available online: https://www.geoengineer.org/publications/online-library?keywords%5B0%5D=Geotechnical%20Enginering%20Circular%20No%207%3A%20Soil%20Nail%20Walls%2C%20Reference%20Manual (accessed on 20 February 2022).
34. Taylor, T.P.; Collin, J.G.; Berg, R.R. *Evaluation of Limit Equilibrium Analysis Methods for Design of Soil Nail Walls*; Report No. FHWA-NHI-17-068; Federal Highway Administration: Washington, DC, USA, 2017; 56p. Available online: https://www.fhwa.dot.gov/engineering/geotech/pubs/nhi17068.pdf (accessed on 20 August 2022).
35. Al-Hussaini, M.M.; Johnson, L.D. Numerical analysis of reinforced earth wall. *Proc. ASCE Symp. Earth Reinf. Pittsburgh* **1978**, 98–126.
36. Jaky, J. The coefficient of earth pressure at rest. In Hungarian (A nyugalmi nyomas tenyezoje). *J. Soc. Hung. Eng. Arch.* **1944**, *78 (22)*, 355–358.
37. Rowe, R.K.; Ho, S.K. Horizontal deformation in reinforced soil walls. *Can. Geotech. J.*,**1998**, *35*, 312–327. https://doi.org/10.1139/t97-062.
38. Vieira, C.S., Lopes, M.L.; Caldeira, L.M.M.S. Influence of facing panel rigidity on performance of reinforced soil retaining walls: A numerical study. *Proc. of the 4th European Geosynthetics Conf. – EuroGeo4.* **2008**, Edinburgh, United Kingdom, pp. 244.
39. Shiu, Y.K.; Chang, G.W.K. Soil nail head review. Geo-Report No. 175, 2005, 106p. Available online: https://www.cedd.gov.hk/eng/publications/geo/geo-reports/geo_rpt175/index.html (accessed on 22 February 2022).
40. Rawat, S.; Zodinpuii, R.; Manna, B.; Sharma, K.G. Investigation on failure mechanism of nailed soil slopes under surcharge loading: Testing and analysis. *Geomech. Geoengin.* **2014**, *9*, 18–35. https://doi.org/10.1080/17486025.2013.804211.